# CHAPTER 124

## FIELD EXPERIMENTS ON A DUAL CYLINDRICAL CAISSON BREAKWATER

* Katsutoshi TANIMOTO*, Hiroshi ENDOH**, Shigeo TAKAHASHI***

### INTRODUCTION

A deepwater caisson breakwater as shown in Fig.1 has been developed by the Ministry of Transport, Japan. The new breakwater is a composite breakwater with a cylindrical caisson named as dual cylinder caisson. The caisson has dual cylindrical walls and its outer cylinder has a perforation in the fore half of the upper portion, forming a wave chamber of a doughnut shape bounded by its inner impermeable cylinder.

A series of laboratory experiments had been carried out at the Port and Harbour Research Institute from 1985 to 1988[1)3)]. According to the laboratory experiments, the caisson was found to have advantages of low reflection and high stability. The design method of the caisson was proposed through intensive laboratory studies in 1988.

Prototype experiments of the dual cylindrical caisson breakwater have been conducted in order to verify its proposed design method against waves at Sakai Port by the Third District Port Construction Bureau, since 1989. A distinguished attempt in the field experiments was tried to measure the displacement of caisson as well as wave pressures during sliding due to high waves. This attempt was accomplished by a storm occurred on February 17, 1991.

Photo 1 shows a scene of the test breakwater after the storm. The middle caisson was slid and fallen down from the rubble mound. The middle caisson is the test caisson which was designed against a

---

* Professor, Faculty of Engineering, Saitama University, Japan
** Former Director General, Kobe Investigation and Design Office, The third District Port Construction Bureau, Ministry of Transport
*** Chief, Maritime Structures Laboratory, Port and Harbour Research Institute, Ministry of Transport

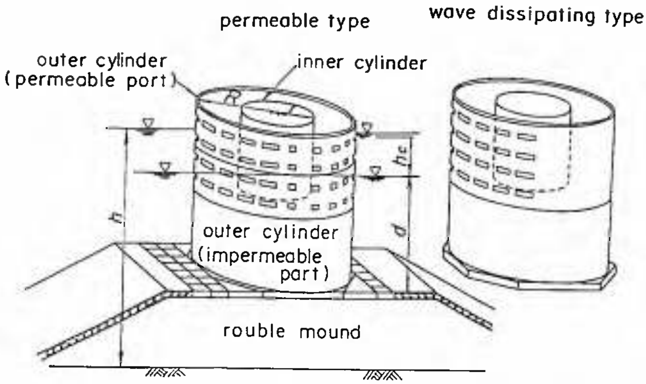


Fig. 1 Conceptual Figure of Dual Cylindrical Caisson

Photo. 1 Slid Caisson in Sakai Port

design wave with one year return period, while the other two caissons were designed with the 50-years return period wave.

After the field test of sliding, model experiments with a scale of 1/21 were performed in a wave basin to reproduce the field situation and investigate the details of the phenomena. The present paper describes both results of field and laboratory experiments, especially on the wave forces and the sliding stability of the caisson in comparison with the proposed design method[4].

## DESIGN OF TEST CAISSON AND MEASURING SYSTEM

### Calculation Method of Design Wave Force

The proposed method to calculate design wave forces and the design of the test caisson for the sliding test are explained here before showing the experimental results.

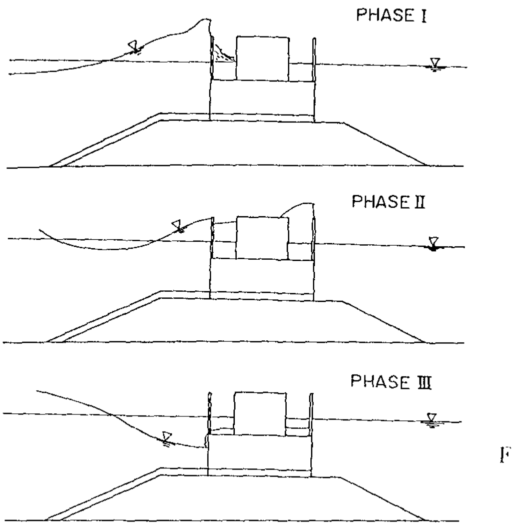


Fig. 2 Three Phases of Wave Action

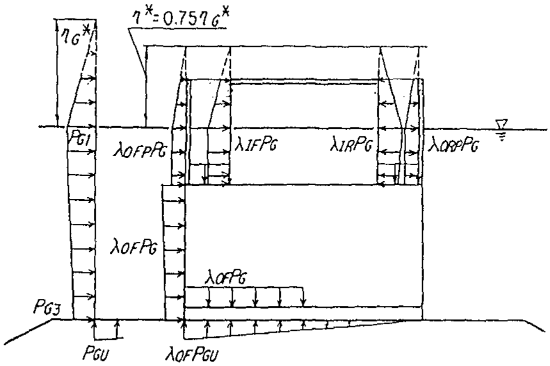


Fig. 3 Distribution of Wave Pressure

Figure 2 demonstrates three phases of wave action which must be considered in the caisson design against waves. The phases 1 indicates the phase when the wave force on the front side of the outer cylinder peaks. At this phase the resultant upward vertical force $F_V$ mostly has its peak during one cycle of wave action and the horizontal wave force on the caisson $F_H$ is large. Consequently, the stability against sliding is most critical at this phase.

The phase II indicates the phase when the wave pressure in the wave chamber is predominant. At this instant, the horizontal wave force $F_H$ peaks, but the vertical force $F_V$ is generally small due to a large amount of seawater in the wave camber. The phase III is when the water surface in front of the caisson is the lowest. The horizontal force has its negative peak ( maximum to the showered) at this phase. The phase II and III are important for the design of the structural strength of the caisson.

A general distribution of the design wave pressure for the phase I and II is shown in Fig. 3. The intensity of wave pressure on each structural member can be obtained from the Goda pressure formula[1)2)] with each modification factor , which had been obtained from the model experiments[3)]. It should be noted that the pressure on the upper half of the outer cylinder in Fig.3 is defined as the difference between the pressures of outer and inner faces of the perforated wall and that the wave pressure is assumed to exert up to the elevation of 0.75 $\eta_G^*$ above the still water level.

The basic pressure distribution is calculated by the Goda pressure formula with $\alpha_2 = 0$ as follows:

$$\eta_G^* = 0.75(1+\cos\beta)H_D \tag{1}$$

$$p_{G1} = 0.5(1+\cos\beta)\alpha_1 w_0 H_D \tag{2}$$

$$p_{G3} = p_{Gu} = \alpha_3 p_{G1} \tag{3}$$

where

$$\alpha_1 = 0.6 + 0.5[(4\pi h / L_D) / \sinh(4\pi h / L_D)]^2 \tag{4}$$

$$\alpha_3 = 1 - (h'/h)[1 - 1/\cosh(2\pi h / L_D)] \tag{5}$$

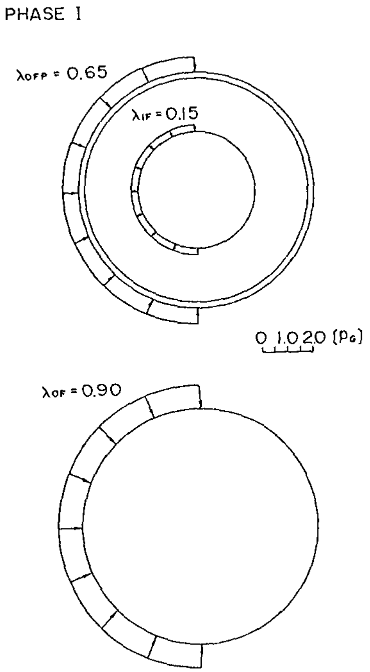


Fig. 4 Wave Pressure Distribution in Horizontal Sections at Phase I

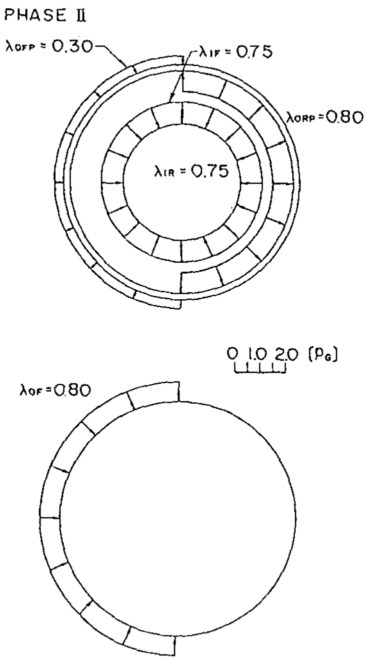


Fig. 5 Wave Pressure Distribution in Horizontal Sections at Phase II

$\beta$ : the angle of wave approach measured from a line normal to the breakwater alignment, $H_D$, $L_D$ : the wave height and length applied to the calculation of design wave forces, $w_o$ : the specific weight of seawater, h : the water depth in front of the breakwater, h' : the distance from the design water level to the bottom of the caisson.

The wave pressure distribution in the horizontal sections and values of the modification factors are shown in Fig. 4 for the phase I. The wave pressure is assumed to act uniformly on the fore half of cylinders for the action of non-breaking waves. The modification factor $\lambda_{OFP}$ for the perforated wall is 0.65, and the modification factor $\lambda_{OF}$ for the lower impermeable part of the outer cylinder is 0.9. The modification factor $\lambda_{IF}$ for the front half of the inner cylinder is 0.15. The modification factors at the phase II are similarly shown in Fig. 5.

The negative wave pressure at the phase III can be obtained appropriately according to the fourth order approximation of a finite amplitude standing wave theory. The residual water level in the wave chamber, however, must be separately given as $\eta^- = 0.25\ H_D$. The pressures in the wave chamber is the hydrostatic water pressure corresponding to the difference between the water level and the still water level.

## Design Condition and Safety Factor Against Sliding

The design wave with a return period of one year was selected for the sliding test caisson. The design conditions are as follows:

$H_{1/3}$ = 2.6 m, $H_D = H_{MAX}$ = 4.7 m ,
$\beta$ = 0 , Design tidal level = + 0.4 m

Figure 6 shows a cross section of the sliding test caisson. The caisson is a reinforced concrete caisson with the outer diameter of 16.2 m and the height of 10.4 m. The opening ratio of the perforated wall is 0.25. The inside of caisson is filled with only water to reduce the caisson weight for the sliding test. The caisson weight deducted the buoyancy in seawater is 860 tf.

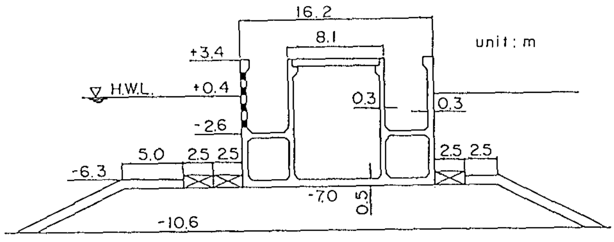


Fig. 6 Cross Section of Sliding Test Caisson

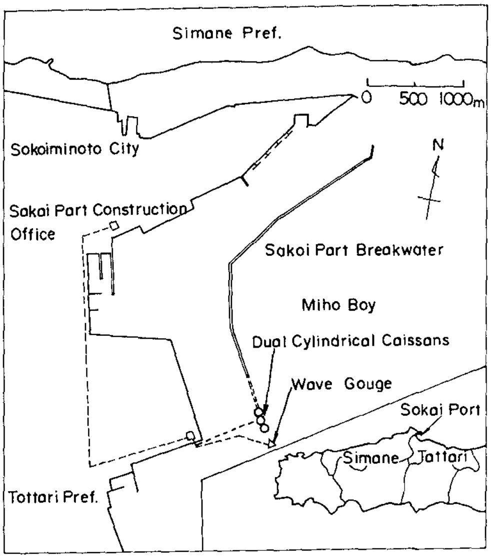


Fig. 7 Test Caissons in Sakai Port

The safety factor $SF_S$ against sliding is defined by the following relation:

$$SF_S = \mu (W_0 - F_V) / F_H \tag{6}$$

where $\mu$ is the friction coefficient between the bottom slab of caisson and the rubble mound foundation, and it is taken as 0.6 according to the design standard of breakwaters. The safety factor of the test caisson is 0.98 against the calculated wave force.

## Measuring System

Figure 7 shows the plan of Sakai Port and the location of the test breakwater. The test breakwater is isolated one consisting of three units of caissons. The middle caisson is the sliding test caisson.

The wave profile and wave direction were measured by a set of wave gauges and velocity meters which located at the position 250 m away from the test breakwater as in the figure. Thirty four pressure transducers were attached to the sliding test caisson to measure the wave pressure distribution and to calculate the resultant wave force. Six displacement meters of wire type were equipped at the top and the bottom of the caisson. They were fixed on the neighboring caissons and on armor concrete blocks for the rubble mound foundation. The data of the pressures and displacements were recorded continuously during storms by a computer in an on-land observation house.

## SOME RESULTS OF FIELD EXPERIMENTS

### Example of Analogue Records

Figure 8 shows an example of field records obtained during the storm in February 17, 1991. The top record indicates the water surface oscillation measured by the wave gage. The middle record indicates the wave pressure profile at the impermeable front wall. It is noticed that the time profile of the pressure is well correlated to that of the water surface elevation. This is because the incident waves to the breakwater are diffracted waves by a peninsula (Zizou-misaki Cape of Shimane Peninshula) and have relatively long crests and the wave angle is almost zero. The bottom record shows the horizontal displacement of the caisson measured at the bottom. The first sliding is not included in this figure and the displacement from the second to the fifth sliding is shown in the figure. The capacity of the displacement meters was

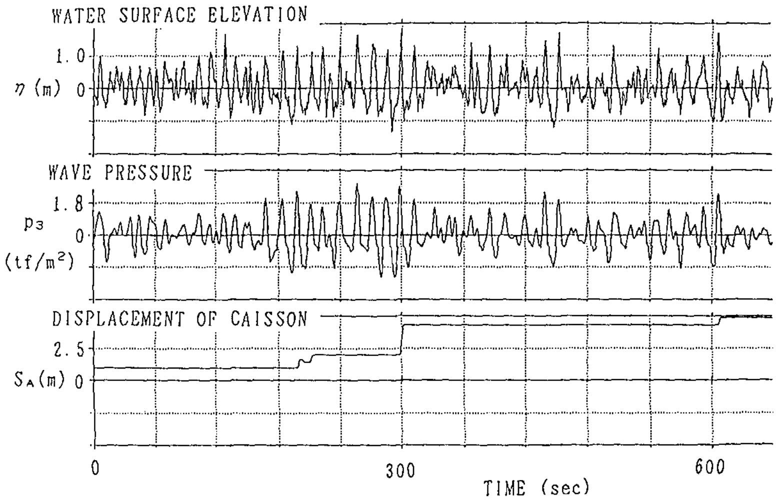


Fig. 8 Sample Record during the Storm on the 17th of February 1991

Table 1 Waves and Sliding Distances

| TIME | $H_{max}$(m) | $H_{1/3}$(m) | $T_{1/3}$(s) | $S_A$(m) | $\Delta S$(m) | |
|---|---|---|---|---|---|---|
| 2:45-3:00 | 3.15 | 2.05 | 14.1 | 1.06 | 1.06 | once |
| 3:00-3:15 | 2.77 | 1.72 | 13.1 | 1.06 | 0 | no |
| 3:15-3:30 | 3.19 | 2.03 | 12.7 | 4.32 | 3.26 | thrice |
| 3:30-3:45 | 2.92 | 2.05 | 12.6 | 4.87 | 0.55 | once |
| 3:45-4:00 | 3.17 | 2.23 | 13.4 | >5 | | |

5 m and therefore, the wires of the meters were cut off when the sixth sliding occurred.

## Wave Conditions and Sliding Distances

The first sliding was recorded at 02:50:40 on February 17 and the sixth sliding was occurred at 03:53:47 on the same day. Observed waves were analyzed for every 15 minutes from 02:45:00 to 04:00:00. The results are shown in Table 1 together with data of the sliding distances, in which $S_A$ denotes an accumulated sliding distance and S denotes the sliding distance during each 15 minutes. For the first 15 minutes, the maximum wave height is 3.15 m, the significant wave height and period are 2.05 m and 14.1 s, and the first sliding occurred which distance was 1.06 m. The tidal level is observed as 0.31 m above the datum level at this time. This sliding distance by one wave is considerably large due to the non breaking wave action having a relatively long wave period in this case.

## Measured Wave Pressure Intensity

Figure 9 demonstrates the order of the magnitude of the wave pressure measured at several points of the caisson. In this figure, the representative positive wave pressure intensities like $p_{max}$, $p_{1/10}$, and $p_{1/3}$ are plotted against the corresponding representative wave heights like $H_{max}$, $H_{1/10}$, and $H_{1/3}$. Relatively large pressure intensities appear at the most rear part in the wave chamber, but the intensity is less than 1.0 $w_0H$.

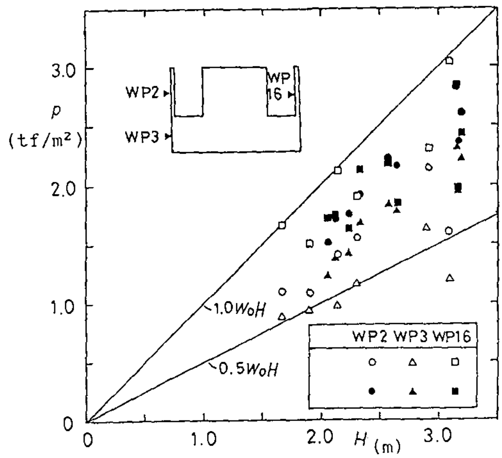


Fig. 9 Pressure Intensities in the Field Experiments

## LABORATORY EXPERIMENTS AND COMPARISON WITH FIELD DATA

### Wave Conditions

Laboratory experiments were carried out to reproduce the field experiment in a wave basin with a model scale of 1/21 using uni-directional irregular waves. Seven kinds of laboratory waves having different wave heights and periods were used in the experiments. Two of them are corresponding to the November storm waves and others are corresponding to the February storm waves, which wave conditions are listed in Table 1. The November storm is a short and small storm just after the completion of the caisson installation. For each of them five different wave trains were prepared. Representative wave parameters according to the zero-upcrossing method are presented in Table 2 with the mean value and the standard deviation for five wave trains. The duration time of one wave train is 15 minutes. The wave direction is perpendicular to the breakwater alignment.

The wave spectra for the November storms are represented by the Modified Bretschneider-Mitsuyasu (MBM) spectrum. For the February storm, however, the MBM spectrum is not applicable, because the observed spectrum is very sharply peaked. Therefore, the JONSWAP type is applied as the target spectrum of the February storm. The peak parameter in the JONSWAP spectrum can be selected so that the realized spectrum coincides with the spectrum observed in the field as much as possible. Figure 10 shows the comparison of the wave spectra in the field and in the laboratory.

Table 2 Waves in Laboratory Experiments

| | Field | | | Laboratory | | |
|---|---|---|---|---|---|---|
| | $H_{max}$(m) | $H_{1/3}$(m) | $T_{1/3}$(s) | $H_{max}$(m) (mean, S.D.) | $H_{1/3}$(m) (mean, S.D.) | $T_{1/3}$(s) |
| II A | 2.91 | 1.90 | 7.1 | 2.56～3.02 (2.84, 0.165) | 1.87～1.93 (1.89, 0.021) | 7.0～ 7.2 |
| II B | 3.09 | 1.67 | 6.4 | 2.47～2.87 (2.64, 0.153) | 1.65～1.68 (1.66, 0.011) | 6.3～ 6.5 |
| II C | 2.62 (3.15)' | 2.05 | 14.1 | 2.76～3.05 (2.86, 0.103) | 1.99～2.09 (2.05, 0.032) | 14.0～14.2 |
| II D | 2.50 (2.77)' | 1.72 | 13.1 | 2.30～2.72 (2.53, 0.135) | 1.69～1.76 (1.72, 0.028) | 13.1～13.3 |
| II E | 2.61 (3.19)' | 2.03 | 12.7 | 2.75～2.93 (2.84, 0.062) | 2.03～2.05 (2.04, 0.006) | 12.6～12.7 |
| II F | 2.74 (2.92)' | 2.05 | 12.6 | 2.73～3.19 (2.95, 0.156) | 2.02～2.08 (2.04, 0.023) | 12.5～12.6 |
| II G | 2.91 (3.17)' | 2.23 | 13.4 | 3.12～3.35 (3.26, 0.091) | 2.18～2.29 (2.22, 0.036) | 13.2～13.3 |

'(zero crossing down)

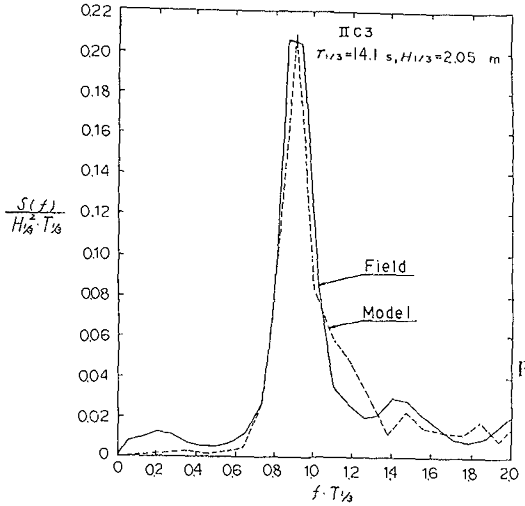


Fig. 10 Wave Spectra in the Field and Laboratory

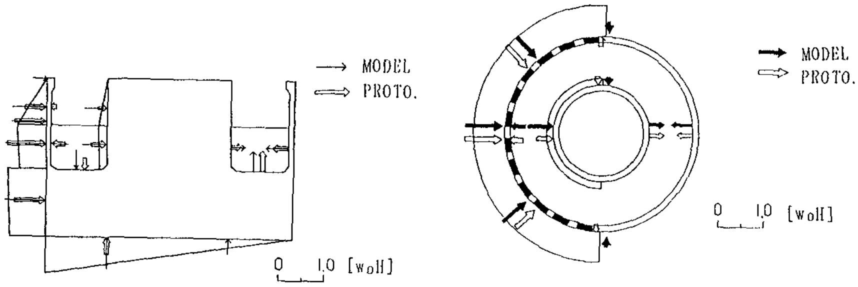


Fig. 11 Measured Instantaneous Pressure Distribution

## Wave Pressure Distribution

Figure 11 shows an example of the instantaneous distribution of wave pressures when the wave force at the phase 1 is the largest during the action of random waves. Both data measured in the field and the laboratory are shown together with the distribution calculated by the proposed method. Although the measured wave pressure are considerably larger than the calculated ones at the front of the inner cylinder, it can be said that the proposed method predicts well the wave pressure distribution as a whole. The resultant wave forces are calculated from such an instantaneous distribution of the wave pressures by considering application areas of caisson walls shared by respective measuring points.

## Horizontal and Vertical Wave Forces

Peak values of measured and calculated wave forces for the phase I are compared in Figs. 12 and 13. In the figures, the ordinate indicates the measured force and the abscissa indicates the calculated force. The horizontal wave forces are shown in Fig. 12, where the measured wave forces in the laboratory experiments are generally larger than the calculated ones, but the laboratory data agree well the field data. Data of the vertical wave forces in Fig. 13 are widely scattered. The main reason is that the amount of water in the wave chamber at the phase I varies considerably depending on the wave periods and wave trains.

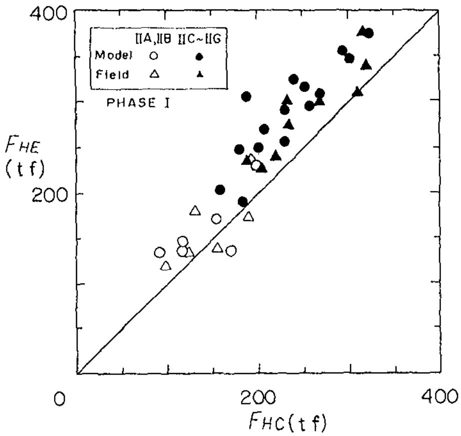


Fig. 12 Horizontal Wave Forces

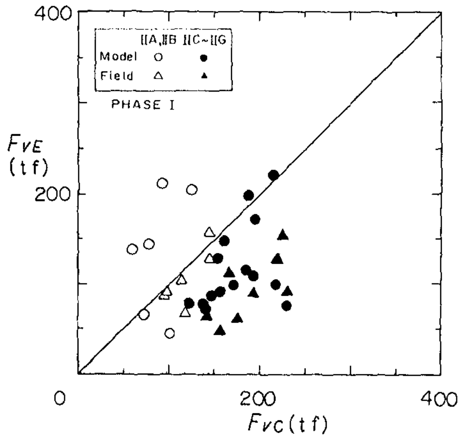


Fig. 13 Vertical Wave Forces

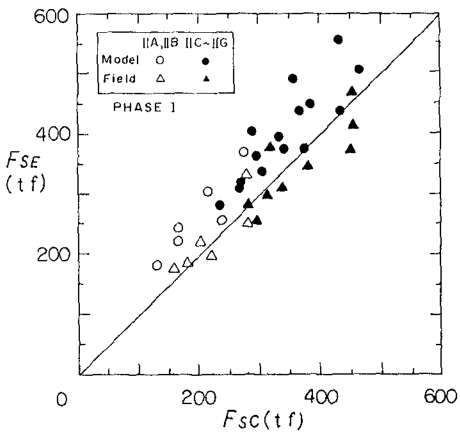


Fig. 14 Equivalent Sliding Forces

Figure 14 shows the peak values of calculated and measured equivalent sliding forces which are equal to $(F_H + \mu F_V)$. The ordinate indicates the measured force and the abscissa indicates the calculated force. The equivalent sliding forces in the laboratory experiments are generally larger than the calculated ones, as the horizontal forces in Fig. 11. However, it should be noted that the equivalent sliding forces measured in the field are a little lower than those in the laboratory and are almost the same as the calculated ones. The measured wave forces scatter significantly in the figures. This is becuase the wave profile varies even though the wave height is the same. Therefore, this may be the reason of the difference between the values in the laboratory and the field.

## Relation between Safety Factor and Sliding Distance

In the laboratory experiments, the horizontal displacement was measured for two possible weights of the sliding test caisson. The one is corresponding to the design weight, and the other is the weight assumed that the water level inside the inner caisson lowers to the tidal level. They are denoted by $W_1$ and $W_2$, respectively. $W_2$ is calculated as 781 tf in a still water and is 90% of $W_1$. Because it is difficult to prevent the leakage of water from the inner cylinder, the weight $W_2$ is presumably the weight during sliding.

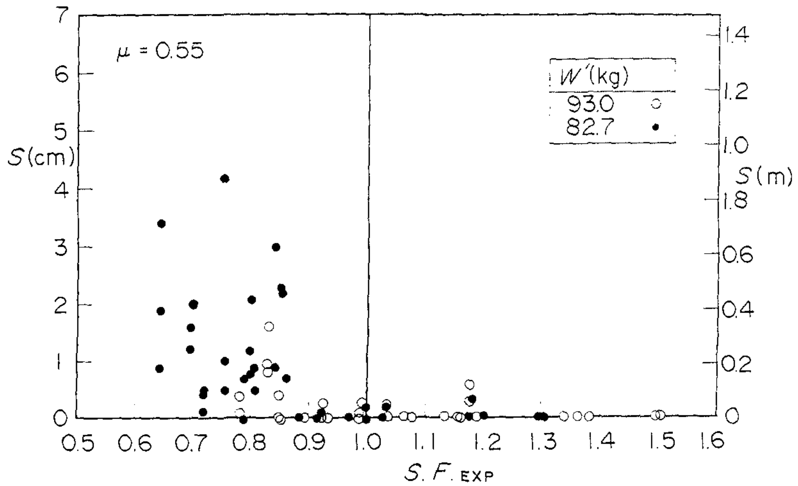


Fig. 15 Safety Factor and Sliding Distance

In the laboratory experiments, the friction coefficient was also measured. Since the sliding in the field occurred only three months after its installation and no large storms attacked the caisson until the sliding occurred, the compaction of the rubble mound by the caisson movements was not enough to get the ordinary friction factor of 0.6. The measured friction coefficient without the compaction of the rubble mound were about 0.55 in the laboratory experiments.

Figure 15 shows the results of sliding tests in the laboratory. The ordinate indicates the maximum sliding distance by one wave during the action of irregular waves. The abscissa indicates the safety factor against sliding, which is calculated for the measured wave forces, the caisson weight ($W_1$ or $W_2$), and the friction coefficient of 0.55. The results shows that the caisson slides in most cases having the safety factor less than 1.0. Thus, the results of laboratory experiments suggests that the occurrence of the sliding can be judged by the safety factor.

Safety Factor against Sliding for the Field Data

The safety factor against sliding which is calculated according to the measured wavc forces is shown in Table 3 for the condition of the first sliding in the field. The caisson slid by 1.06 m during the first sliding. The safety factor is 0.93, less than 1.0, when the friction factor is assumed to be 0.55 and the caisson weight is $W_2$. Even if the caisson weight is $W_1$ and the friction factor is 0.6, the safety factor is less than 1.2. Therefore, it can be concluded that the caisson sliding can be judged by its safety factor also in the field experiments.

Table 3 Safety Factor against Sliding

| $w_0$(tf) | $\mu$ | S.F. |
|---|---|---|
| 895 | 0.60 | 1.19 |
| 895 | 0.55 | 1.10 |
| 781 | 0.60 | 1.01 |
| 781 | 0.55 | 0.93 |

The safety factor using the calculated wave forces, the caisson weight of $W_2$ and the friction coefficient of 0.55 is 0.87. Because the measured wave forces in the field are almost the same as the calculated wave forces, the safety factor against sliding using the calculated wave forces is close to that using the measured wave forces.

## CONCLUDING REMARKS

Slidings of a prototype dual cylinder caisson were successfully measured in the field verification experiments. The slidings of the caisson were reproduced in laboratory experiments. The major conclusions in this study are as follows:

1)The sliding of the caisson can be judged by its safety factor using the measured wave forces, the caisson weight and the friction factor both in the field and in the laboratory.

2)The measured wave forces acting on the caisson in the field were almost the same as the calculated wave forces. Therefore, the sliding of the caisson in the field can be judged also by the safety factor using the calculated wave forces.

3)The measured wave forces in the laboratory are larger than those in the field as a whole. However the difference is not significant and this is because of the wide variation of the laboratory data.

## ACKNOWLEDGMENTS

The field experiments have been conducted under the guidance of the advisory committee chaired by professor Y. Goda. The experiments were carried out by the collaboration with many engineers especially of the Sakai Port Construction Office and the Kobe Design and Investigation Office of the Third District Port Construction Bureau, MOT. The authors wish to express their sincere gratitude to all the people.

## REFERENCES

1) TANIMOTO, K., TAKAHASHI, S., and KIMURA, K. : Structures and Hydraulic Characteristics of Breakwaters, - State of the Art of Breakwater Design in Japan-. Rept. of Port and Harbour Res. Inst., Vol. 26, No. 5. 1987, pp. 11-55.

2) GODA, Y. : Random Seas and Design of Maritime Structures, University Tokyo Press, 1985, 323 p.

3) TANIMOTO, K., et al. : Hydraulic Characteristics and Design Wave Forces of Double-Cylindrical Caisson, - A Study on Development of Deepwater Breakwater (part 4) - , Tech. Note of Port and Harbour Res. Inst., No. 600, 1987, pp. 1-21, (in Japanese).

4) TAKAHASHI, S., Ken'ichirou SHIMOSAKO, and Hitoshi SASAKI : Experimental Study on Wave Forces and Sliding of Dual Cylinder Caisson - Reproducing Experiment of Field Sliding Test in Sakai Port-., Tech. Note of Port and Harbour Res. Inst., No. 742, 1992, (in Japanese).